Inorganic Chemistry

Article

pubs.acs.org/IC

Synthesis of Ternary and Quaternary Graphite Intercalation Compounds Containing Alkali Metal Cations and Diamines

Tosapol Maluangnont,[†] Michael M. Lerner,*[,†] and Kazuma Gotoh[‡]

[†]Department of Chemistry, Oregon State University, Corvallis, Oregon 97331-4003, United States

[‡]Department of Chemistry, Faculty of Science, Okayama University 3-1-1 Tsushima-naka, Kita-ku, Okayama City 700-8530, Japan

ABSTRACT: A series of ternary graphite intercalation compounds (GICs) of alkali metal cations (M = Li, Na, K) and diamines [EN (ethylenediamine), 12DAP (1,2-diaminopropane), and DMEDA (*N*,*N*-dimethylethylenediamine)] are reported. These include stage 1 and 2 M–EN–GIC (M = Li, d_i = 0.68–0.84 nm; M = Na, d_i = 0.68 nm), stage 2 Li–12DAP–GIC (d_i = 0.83 nm), and stage 1 and 2 Li–DMEDA–GIC (d_i = 0.91 nm), where d_i is the gallery height. For M = Li, a perpendicular-to-parallel transition of EN is observed upon evacuation, whereas for M = Na, the EN remains in parallel orientation. Li–12DAP–GIC and Li–DMEDA–GIC contain chelated Li^+ and do not show the perpendicular-to-parallel transition. We also report the quaternary compounds of mixed cations (Li,Na)–12DAP–GIC and mixed amines Na–(EN,12DAP)–GIC, with d_i values in both cases between those of the ternary end members. (Li,Na)–12DAP–GIC is a solid solution with lattice dimensions dependent on composition, whereas for Na–(EN,12DAP)–GIC, the lattice dimension does not vary with amine content.

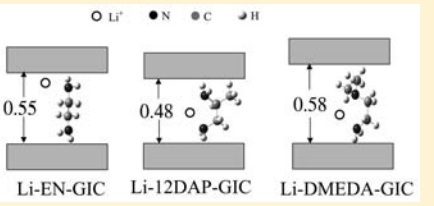

INTRODUCTION

Intercalation, i.e., the insertion of guest species into layered host materials, can result in changes in both structures and properties of the layered host and guest.[1] Intercalation compounds have numerous applications, including the adsorption of toxins, use as photo and electro-functional materials, or use as precursors in the formation of clay–polymer nanocomposites with enhanced mechanical properties.[2] Large guests can generate microporosity within layered solids; one proposed related application for graphite intercalation compounds (GICs) lies in hydrogen storage.[3,4] Other intercalation reactions can be used to facilitate the exfoliation of hosts into individual sheets. Besides the interesting properties of the single-sheet structures themselves, the delamination is a key step toward reassembled materials with novel magnetic, optical, and electronic properties.[5,6] A fundamental understanding of intercalation compositions, energetics, and intragallery structures will enable new routes to expanded or exfoliated materials and to designed materials with desirable properties.

The exfoliation of graphite to form single-layer graphene sheets may be the key to their large-scale synthesis, and this method has received a great deal of attention. Recent reports describe the use of binary or ternary GICs as precursors in graphene production through low-temperature, liquid phase exfoliation. The intercalates studied include potassium,[7−9] K/THF,[10] bromine,[11] $FeCl_3/CH_3NO_2$,[9] and Na/NH_3.[12] A broader understanding of GIC chemistry may facilitate the success of this approach.

The α,ω-diamines, $H_2N(CH_2)_xNH_2$, have been widely employed as intercalate guests, with hosts including metal (hydrogen/oxo)phosphates, metal chalcogenides, metal oxychlorides, metal oxides, and clays.[1] The incorporation of diamines into a three-dimensional host structure such as zeolite ZSM-5, and Y is also known.[13] In addition to the parallel or perpendicular orientations that are observed with monoamine analogs, the presence of two functional groups can result in more complex intragallery arrangements for diamines. For example, different bonding modes of diamines intercalated into graphite oxide (GO) have been proposed.[14] These include (i) bridging two different layers, (ii) looping the two active sites on the same layer, and (iii) tailing where only one amine is strongly bound.

The number of GICs prepared containing diamines is surprisingly limited. In donor-type GICs, the graphene sheets are reduced, and cations intercalate to maintain charge neutrality.[15−17] Ternary GICs are produced when the metal cations intercalate as solvated ions. The stage 2 compound Li–EN–GIC (EN = ethylenediamine) was prepared by Rüdorff[18] by the direct reaction of graphite, EN, and Li metal. However, the orientation of EN within the intercalate galleries was not described. Later, Merle et al.[19] prepared K–TMEDA–GIC (TMEDA = *N*,*N*,*N*′,*N*′-tetramethylethylenediamine) by the ternarization of KC_{24} with TMEDA. More recently, we reported the preparation of M–12DAP–GICs (M = Li, Na, K; 12DAP = 1,2-diaminopropane).[20] A GIC containing the macrocylic cyptand "222" (4,7,13,16,21,24-hexaoxa-1,10-diazabicyclo[8.8.8]hexacosane)[21] has also been reported.

In addition to these diamine intercalates, there are several known GICs containing monoamines, including ammonia,[22−24] methylamine,[25] and triethylamine.[19] We added several to this list by reporting a homologous series of ternary GICs containing Na^+ solvated by *n*-alkylamines with *x* carbon atoms, Na–*n*C*x*–GIC (*x* = 3, 4, 6, 8, 12, and 14).[26] A recent study also compared the

Received: August 1, 2011
Published: October 19, 2011

Scheme 1. Structure of the Diamines and Abbreviations Used in This Work

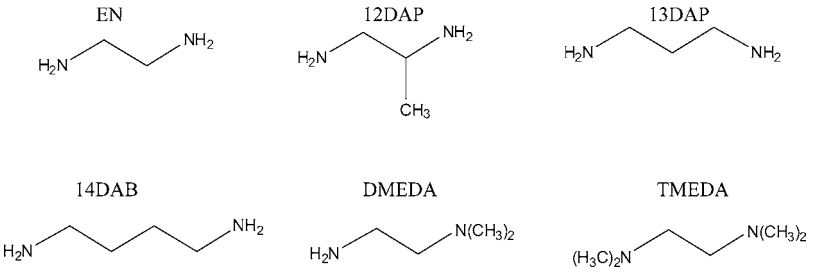

structures of GICs containing alkali metals and linear vs branched amines.[27]

The rich structural chemistry of ternary M−amine−GICs can be expanded by employing the mixture of alkali metal cations or of the mixed amines, resulting in the quaternary compounds. The only donor-type quaternary GICs containing two metal cations and an organic cointercalate that we are aware of is $MHg(benzene)_2C_8$ (M = K, Rb),[28] which displays a heterostructure of the sequence C−M−Hg−M−C−benzene−C along the stacking direction. Quaternary GICs with two organic intercalates include Li−(THF,BzN)−GIC[29] and K−(THF,Bz)−GIC[30] (THF = tetrahydrofuran, Bz = benzene, BzN = benzonitrile).

In this article, we describe several new GICs containing alkali metal cations (M = Li, Na, K) with diamines. We will describe the gallery structure and composition for the different cations as well as varying (i) diamine carbon chain lengths, i.e., x in $H_2N(CH_2)_xNH_2$, (ii) methyl substitution at the amine, i.e., $-NH_2$ vs $-N(CH_3)_2$, and (iii) structural isomerism such as in $H_2N(CH_2)_3NH_2$ vs $H_2NCH_2CH(NH_2)CH_3$. We also report herein the synthesis, structural features, and kinetics of the quaternary compounds (Li,Na)−12DAP−GIC and Na−(EN,12DAP)−GIC.

EXPERIMENTAL SECTION

All synthesis and handling of the air-sensitive reagents and the resulting GICs were performed under an inert atmosphere (N_2 for Na, K; Ar for Li) using a drybox or septum-syringe techniques. Amines were dried over a molecular sieve 4A prior to use. The structures of the amines employed, including their abbreviations, are shown in Scheme 1. In a typical synthesis of stage 1 compounds, 0.25 g (21 mmol) of polycrystalline graphite powder (SP-1, Union Carbide, average particle diameter 100 μm) was mixed with 0.060 g of Na metal (99.95%, Alfa Aesar; 2.6 mmol) and the amine (2 mL).

Caution! *Alkali metals are highly flammable when in contact with air and/or water and should be handled with care.*

The reaction mixtures were vigorously stirred at 70 °C for the following periods: Na−EN−GIC (24 h), Na−12DAP−GIC (72 h), Li−12DAP−GIC (6 h), and Li−DMEDA−GIC (12 h). Li-containing products were obtained using similar methods, but with increased metal reagent amounts and long reactions times. For example, the stage 1 Li−EN−GIC was reproducibly produced using 0.030 g (4.3 mmol) of Li and a 72 h reaction.

Caution! *Pressure in these reactors may increase and must be vented.*

To synthesize stage 2 compounds, the above-mentioned conditions were optimized as follows: Na−EN−GIC (0.010 g of Na, 0.4 mmol, 72 h), Li−EN−GIC (0.010 g Li, 1.4 mmol, 72 h), Li−12DAP−GIC (5 mL of 12DAP, intermittent stirring), and Li−DMEDA−GIC (150 h). The synthesis of Li−DMEDA−GIC is poorly reproducible.

The quaternary (Li,Na)−12DAP−GIC was synthesized by employing 2.6 mmol of each metal to react with graphite and 12DAP. The quaternary Na−(EN,12DAP)−GIC was synthesized starting from 0.25 g of dry stage 2 Na−EN−GIC with 2.6 mmol of Na and 2 mL of 12DAP. The mixtures were reacted for 0.5−72 h. The liquid amines were removed by centrifugation immediately, and the GIC products were rinsed briefly with the amine. GIC products denoted "as prepared" were characterized after centrifugation and brief washing without further processing; other samples were placed under a vacuum (<100 μm) at 60 °C for 6 h. Different drying conditions were applied for Li−EN−GIC (as described below).

Powder X-ray diffraction (PXRD) data were collected on a Rigaku MiniFlex II, using Ni-filtered Cu Kα radiation, with 0.02° 2θ steps from 5° to 35°. Sample holders were sealed with a plastic tape window to prevent decomposition in the air during the PXRD measurement. The (00L) reflections were indexed according to the relation $I_c = d_i + (n - 1)(0.335\ \text{nm})$, where I_c is the identity period obtained directly from diffraction data, d_i is the gallery height, n is the GIC stage number, and 0.335 nm is the distance between two adjacent graphene sheets. The gallery expansion, Δd, is defined as $\Delta d = d_i - 0.335$ nm. Figure 1a illustrates these dimensions schematically.

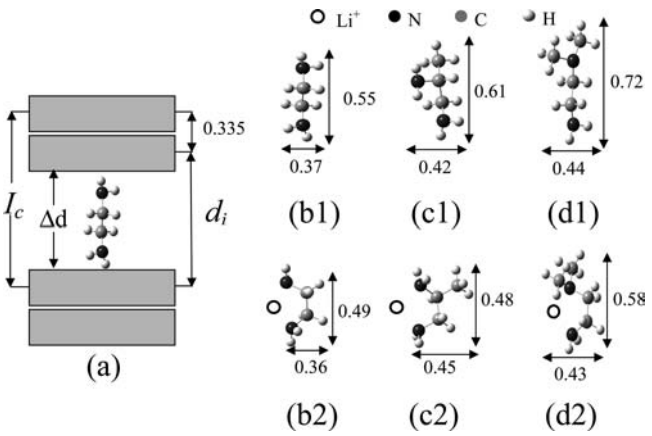

Figure 1. (a) Structural parameters used to describe GICs, shown here as stage 2, and calculated dimensions in nanometers of (b) EN, (c) 12DAP, and (d) DMEDA. Labels 1 and 2 indicate bonding in the head-to-tail (monodentate) and chelation (bidentate) modes, respectively.

Thermogravimetric analysis (TGA) was performed with a Shimadzu TGA-50 under flowing Ar gas (20 mL/min) from RT to 800 at 5 °C/min. Elemental analyses for alkali metals were performed after alkali cations in GICs were extracted into the liquid phase by a gentle boiling in 3:1 (v/v) HCl/HNO_3 as described previously.[27] Capillary zone electrophoresis (CZE) on the extract solutions was performed using an Agilent Technologies HP^{3D}CE equipped with a UV detector, a fused-silica capillary, and indirect detection at 210 nm. Separation was accomplished at 30 °C with an applied voltage of +15 kV, employing the background electrolyte (pH = 5.2, adjusted with glacial acetic acid) of 15 mM imidazole in water. Metal contents were quantified using a calibration curve obtained from the peak areas of the cations' standard solutions (0.1−1.0 mM).[27] GICs synthesized from different batches and separately analyzed showed amine contents agreeing within 2%, and the alkali metal contents within 0.1% (Na) and 3% (Li). ^{1}H NMR spectra were recorded at 299.947 MHz at RT using a Varian

dx.doi.org/10.1021/ic201661y | Inorg. Chem. 2011, 50, 11676−11682

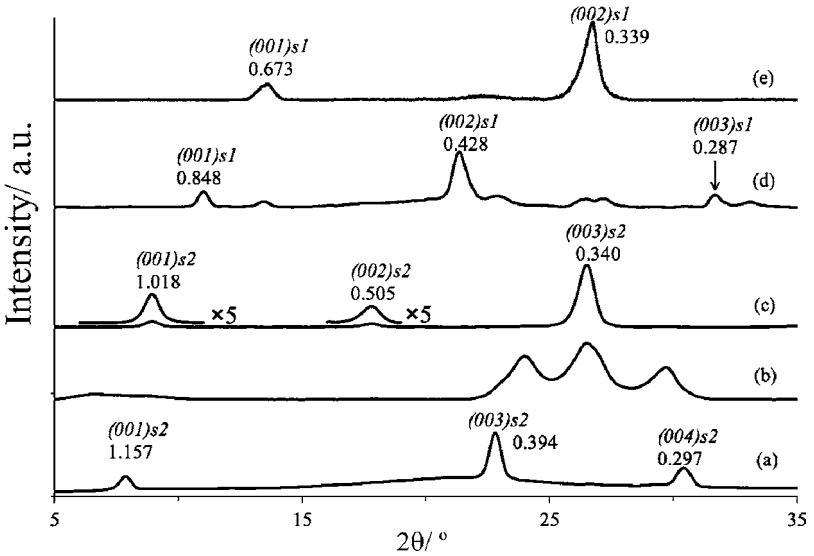

Figure 2. PXRD patterns of Li–EN–GICs: (a) stage 2 as prepared, (b) after 3 h and (c) 6 h of evacuation at 60 °C, (d) stage 1 as prepared, and (e) after 6 h of evacuation at 60 °C. The *d* values (in nm) and assigned Miller indices (00*L*) are indicated for each reflection. The labels s1 and s2 refer to stages 1 and 2, respectively.

(Agilent Technologies) INOVA 300 NMR spectrometer. Samples were sealed in a Zirconia rotor under Ar gas.

The amine cointercalate structures were optimized using the hybrid density functional method (B3LYP) with a 6-31+G(d,p) basis set and the Gaussian 3.0 software.

RESULTS AND DISCUSSION

GICs of Ethylenediamine. Figure 2a,d show PXRD patterns of wet blue/black products obtained by reacting graphite with Li metal and EN. Following Rüdorff,[18] these products can be assigned as stage 2 Li–EN–GIC (I_c = 1.176 nm, d_i = 0.841 nm vs the reported d_i of 0.85 nm[18]) and stage 1 (d_i = 0.855 nm, not reported previously). The stage 1 Li–EN–GIC is prepared by employing 4.3 mmol of Li (instead of 1.4 mmol for stage 2) while fixing the amount of graphite at 21 mmol. The gallery expansions for both stages, $\Delta d \sim 0.5$ nm, agree with the calculated dimension of EN with a perpendicular orientation relative to the graphene sheets. The head-to-tail and chelate structures, Figure 1b1,b2, respectively, have similar dimensions with this orientation, and either fits well with the observed dimensions.

Following evacuation at 60 °C, the stage 1 and 2 phases undergo a structural change and transform into phases with smaller gallery dimensions (d_i = 0.676 and 0.684 nm respectively, $\Delta d \sim 0.35$ nm), as shown in Figure 2b,c,e. From the diamine steric requirements, these phases must have the EN oriented parallel to the graphene sheets. Hence, Li–EN–GIC in Figure 2b is a mixture of phases with perpendicular or parallel orientation of EN. Again, the head-to-tail and chelate structures have similar dimensions with this orientation, and either fits well with the observed dimensions. The expansion observed for the parallel orientation also agrees well with the known monolayer thickness of amines in related GICs, such as Na–*n*-alkylamine–GIC,[26] and in other host structures, such as TiOCl and VOCl[31] or TaS_2.[32] In the case of graphite oxide (GO),[14] EN is also in parallel orientation, and by varying *x* in $H_2N(CH_2)_xNH_2$, the interlayer distance of graphite oxide increases slowly from 0.64 nm (pristine GO) to 0.84 nm (*x* = 4) to 0.99 nm (*x* = 10). GO and amines interact via functional groups on GO, which is different from the redox intercalation in donor-type GICs.

In comparing the related ternary GICs, Li–$H_2NCH_2CH_2X$–GICs with X = CH_3 (*n*-propylamine),[26] X = CH_2CH_3 (*n*-butylamine),[26] and X = NH_2 (EN), only the latter shows the perpendicular-to-parallel transition after evacuation. The other GICs always retain a parallel intercalate orientation.

The cation plays a significant role in directing the orientation of the organic cointercalates in M–EN–GIC. Figure 3a,b shows the PXRD pattern of the stage 1 (d_i = 0.691 nm) and stage 2 (d_i = 0.676 nm) Na–EN–GIC. The as-prepared and evacuated GICs both show $\Delta d \sim 0.36$ nm, indicating a parallel EN orientation. These M–EN–GICs (M = Li, Na) provide another example where a strong cation directing effect occurs, the other reported cases are for M–THF–GIC[33] [d_i = 0.89 nm (M = K); 0.71 nm (M = Cs)], M–N_2–GIC[34] [d_i = 0.957 nm (M = K); 0.946 nm (M = Cs)], and M–12DAP–GIC[20] [d_i = 0.78 nm (M = Li); 0.75 nm (M = Na); 0.70 nm (M = K)]. In all of these cases, counter to the relative cation radii, the gallery dimensions decrease from Li^+ to K^+.

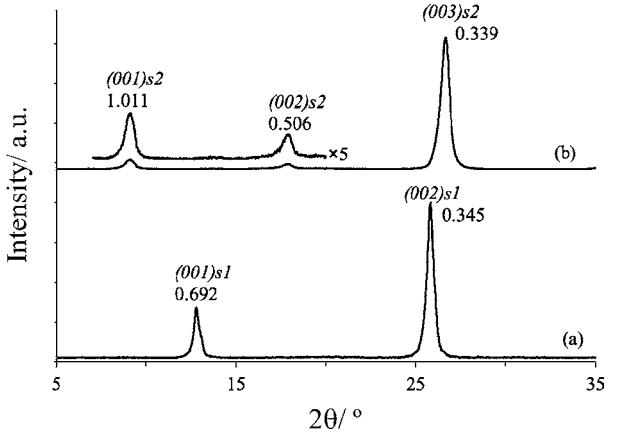

Figure 3. The PXRD patterns of (a) stage 1 and (b) stage 2 Na–EN–GIC. The *d* values (in nm) and assigned Miller indices (00*L*) are indicated for each reflection. The labels s1 and s2 refer to stages 1 and 2, respectively.

dx.doi.org/10.1021/ic201661y | Inorg. Chem. 2011, 50, 11676–11682

Reaction of graphite, K, and EN produces a blue solid product at RT and a black product at 70 °C. In both cases, the product shows only the *weak* (002) of graphite (not shown). It appears that the highly reactive K metal leads to an unstable or amorphous product. Schlögl and Boehm[35] reported that K−THF−GIC decomposed in the mother liquor upon prolonged contact. Alternately, the formation of the EN-solvated K^+ complexes, while known,[36] is less favorable than for Li^+ or Na^+, and this may prevent the formation of an ordered GIC product.

GIC of Substituted Ethylenediamine. The PXRD pattern of Li−12DAP−GIC stage 2 (d_i = 0.827 nm) is shown in Figure 4a. The stage 1 of this GIC was previously

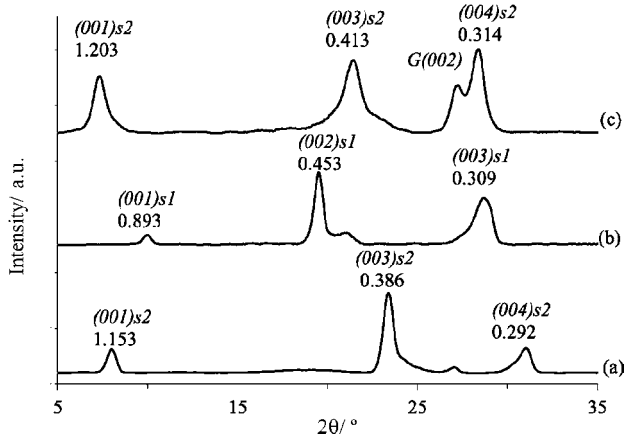

Figure 4. PXRD patterns of (a) stage 2 Li−12DAP−GIC and (b) stage 1 and (c) stage 2 Li−DMEDA−GIC. The *d* values (in nm) and assigned Miller indices (00*L*) are indicated for each reflection. The labels s1 and s2 refer to stages 1 and 2, respectively. *G*(002) indicates the graphite (002) reflection.

reported with a similar gallery dimension.[20] The gallery expansion Δd of 0.48−0.49 nm is in agreement with the calculated dimension of 12DAP perpendicular to the graphene sheets and chelating the cation, Figure 1c2.[20] The calculated dimension of 12DAP without chelation (i.e., along the N−C−C−C backbone), 0.61 nm, is too large. The as-prepared and evacuated products are similar; thus, the added methyl group on the amine (Li−12DAP−GIC compared to Li−EN−GIC) prevents intercalate reorientation. On the other hand, the observed dimensions for K−12DAP−GIC (d_i = 0.697 nm) require that the 12DAP lie parallel to the graphene sheets, whereas in Na−12DAP−GIC (d_i = 0.749 nm), the diamine displays an intermediate orientation.[20]

Ternary GICs of alkali metals with 13DAP and 14DAB are not obtained by these methods; in all trials, only the (002) reflection from graphite is observed after reaction (PXRDs not shown). This underlines the necessity of $-NH_2$ groups in the 1,2 position (i.e., vicinal) for intercalation to proceed. Li metal does not appear to react with and dissolve into 13DAP and 14DAB, whereas Na metal and K metal react but do not generate reactive free radicals. The formation of $M^+H_2N(CH_2)_3NH^-$ from 13DAP was reported in the presence of ultrasound (M = Na) or ammonia gas (M = K).[37] Further, Laszlo et al.[38] showed by ^{23}Na NMR that the preference for Na^+ solvation by the diamines was in the order 14DAB < 13DAP < EN. Ternary GIC formation is, in part, driven by the solvation enthalpy of cointercalates, and this provides another explanation for the instability of GICs containing these diamines.

Figure 4b shows the PXRD pattern of the product assigned as a stage 1 Li−DMEDA−GIC, d_i = 0.910 nm. As-prepared and evacuated products are similar. DMEDA is structurally related to EN with two additional methyl groups substituted for the two hydrogen atoms on the same amine group. The gallery expansion of $\Delta d \sim 0.58$ nm indicates a perpendicular and chelating DMEDA orientation, similar to that observed for EN and 12DAP, Figure 1d2. Stage 2 Li−DMEDA−GIC [d_i = 0.916 nm, Figure 4c], again with perpendicular, chelating DMEDA, was obtained at longer reaction times. Thus, methyl substitution on EN to form 12DAP or DMEDA results in chelation of Li^+ within the GICs and the inhibition of the perpendicular-to-parallel transition.

Although the solvation of Na^+ by DMEDA is known in the solid state,[39] the Na and K analogs of M−DMEDA−GIC were not obtained. The PXRD pattern from the reaction of graphite, Na metal, and DMEDA shows only the unreacted graphite and Na metal remaining in the reaction tube. A similar result was obtained for K metal, though the DMEDA turned brown, indicating solvent decomposition.

The synthesis of a stage 1 K−TMEDA−GIC (d_i = 0.894 nm) by the ternarization of the KC_{24} with TMEDA is known.[19] Assuming the parallel arrangement of TMEDA, the reported Δd = 0.559 nm is close to that observed (0.563 nm) for intercalation compounds of VOCl and TMEDA.[31] We found that the direct reaction of graphite, K metal, and TMEDA yields a blue product with I_c = 0.855 nm (PXRD not shown), and this phase is assigned as K−TMEDA−GIC following Merle et al.[19] Neither Li nor Na metal dissolve in TMEDA, and neither metal produces GICs using this method. The addition of electron transfer agents (e.g., anthracene, biphenyl, naphthalene), known to assist the formation of ternary GICs of alkali metal cations and ether,[40,41] does not result in GIC products. The synthetic obstacles for M−TMEDA−GIC (M = Li, Na, K) by the direct method are not due to the instability of metal TMEDA complexes; many known crystal structures show TMEDA solvating Li^+,[42−46] Na^+,[46−48] or K^+.[49,50]

The formation of radicals/anions/solvated electrons through the reaction of alkali metal with liquid ammonia or small chain amines is well-established in the literature.[51] After reaction with *n*-butyl lithium, free radicals were detected by electron paramagnetic resonance (EPR) for EN and 12DAP, whereas 13DAP and DMEDA were EPR-silent.[52] This is in line with the production of ternary GICs of alkali metals with EN and 12DAP, but nonreaction of 13DAP. Contrary to this model, DMEDA does form GICs. This might be related to the use of Li metal as the reducing agent, rather than *n*-butyl lithium.

Compositional Analyses. ^{1}H static NMR spectra of Na−EN−GIC and EN liquid as a reference are shown in Figure 5. Only a broad signal of EN is observed in Na−EN−GIC; there are no sharp CH_2 and NH_2 peaks of liquid EN at 0.8 and 0.5 kHz. The motion of intercalated EN molecules is restricted, and no excess liquid EN, for example, on the GIC surface, is observed.

Representative mass loss curves for the GIC products obtained are shown in Figure 6. All show mass losses from 50 to 200 °C, followed by a higher temperature mass loss with an onset around 600 °C. The lower temperature loss is ascribed to intercalate volatilization and the latter to the decomposition of the graphitic host lattice. This high temperature mass loss is also observed for a graphite control sample (not shown) and is due to the presence of trace O_2 in the flow gas. The diamine

dx.doi.org/10.1021/ic201661y | *Inorg. Chem.* 2011, 50, 11676−11682

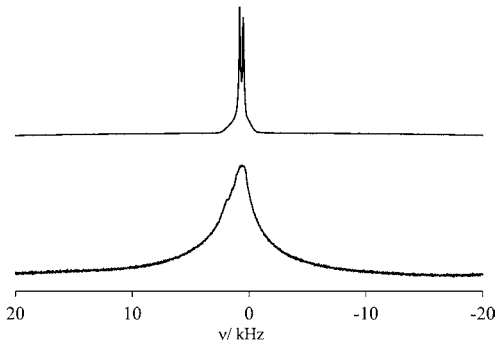

Figure 5. ^{1}H static NMR spectra of Na–EN–GIC and liquid EN (TMS = 0 kHz).

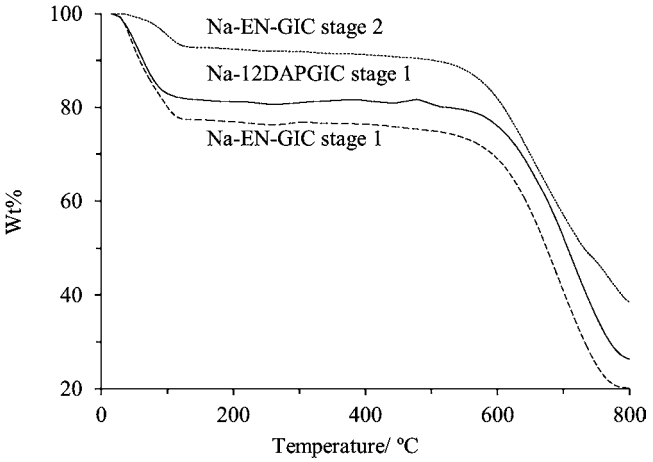

Figure 6. TGA mass loss data for GIC products.

content was determined from the mass loss from 50 to 200 °C and metal content from elemental analyses as described above. GIC compositions thus obtained are provided in Table 1. Assuming that only Na_2O remains after high temperature thermolysis of the Na-containing GICs, the TGA residual masses confirm the metal contents obtained from CZE (for example, 7 wt % Na (from TGA residue) vs 6.5 wt % Na (from CZE) for stage 2 Na–EN–GIC).

The diamine/M molar ratios are generally close to 1:1 similar to, e.g., Na–*n*-propylamine–GIC[26] and others.[53] The composition of the stage 2 perpendicular $Li_1(EN)_{0.7}C_{26}$ found is similar to the reported $Li_1(EN)_{1.0}C_{28}$.[18] The T_d geometry around solvated Li^+ is documented in other GICs such as Li–THF–GIC[54] or Li–DME–GIC.[55] However, the molar ratios found above indicate lower coordination numbers for GICs with diamine intercalates. For most products obtained, the compositions of these ternary GICs are close to one metal cation for 15 (or 26) for stage 1 (or stage 2) graphene C atoms.

The packing fractions within the intercalate galleries are obtained by comparing the experimentally obtained compositions and structural data. For example, with Li–EN–GIC, the values required are the volume of Li^+ (0.0016 nm^3); the van der Waals molar volume of EN (0.0651 nm^3);[56] the surface area per C atom in a graphene layer (0.0261 nm^2); and the experimentally determined GIC composition, stage number, and intercalate gallery expansion. The packing density, or fraction of volume in the expanded galleries occupied by intercalates, can then be determined as

$$[(0.0016\ \text{nm}^3 + (0.7)(0.0651\ \text{nm}^3))/[(26/2)(0.0261\ \text{nm}^2)(0.505\ \text{nm})] = 0.28$$

The calculated packing fractions are shown in Table 1 and fall in the range ~0.2–0.5. These values show a wide range for other ternary GICs, from about 0.1–0.7.[19,22,25–27]

Quaternary GIC with Two Metal Cation Cointercalates. Solid solutions of Li,Na–amine–GIC can be prepared directly by the reaction of graphite with two alkali metals and the amine. PXRD patterns of products from different reaction times are shown in Figure 7 and compositional results in Table 2.

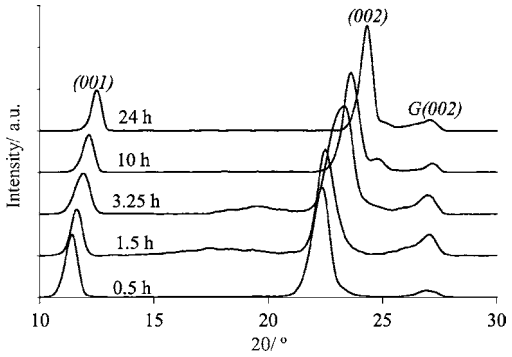

Figure 7. Selected PXRD patterns of the stage 1 (Li,Na)–12DAP–GIC made by direct synthesis at different reaction times. The assigned Miller indices (00*L*) are indicated for each reflection. *G*(002) indicates the (002) reflection from graphite.

In all cases, quaternary stage 1 GICs are obtained. A gradual shift in d_i (in nm) with reaction time is observed: 0.806 (0.5 h), 0.802 (1.5 h), 0.775 (3.25 h), 0.768 (6 h), 0.766 (10 h), and 0.743 (24 h). The shorter reaction times show gallery dimensions closer to those of Li–12DAP–GIC (d_i = 0.816 nm), whereas long reaction times show dimensions more similar to those of

Table 1. Compositional Data for Ternary M–Diamine–GICs

diamine	cation M	stage no.	wt% M	wt% diamine	composition	packing fraction
EN	Li	2	1.72	14.9	$Li_1(EN)_{1.0}C_{28}$[a]	0.35
	Li	2	1.95	11.2	$Li_1(EN)_{0.7}C_{26}$	0.28
	Li	1	2.96	20.8	$Li_1(EN)_{0.8}C_{15}$	0.40
	Na	2	6.50	10.0	$Na_1(EN)_{0.6}C_{25}$	0.40
	Na	1	8.66	21.7	$Na_1(EN)_{1.0}C_{15}$	0.51
12DAP	Li	1	2.82	28.7	$Li_1(12DAP)_{0.95}C_{14}$	0.45
	Li	2	1.76	17.7	$Li_1(12DAP)_{0.94}C_{26}$	0.47
	Na	1	5.70	24.2	$Na_1(12DAP)_{1.3}C_{24}$	0.44

[a]Ref 18.

dx.doi.org/10.1021/ic201661y | *Inorg. Chem.* 2011, 50, 11676–11682

Table 2. Structural and Compositional Data of the Quaternary (Li,Na)−12DAP−GIC

time/h	wt % (metal)	wt % diamine	derived composition
0.5	3.12 (Li), not detected (Na)	29.8	$Li_1(12DAP)_{0.9}C_{12}$
1.5	3.52 (Li), 0.24 (Na)	28.5	$(Li_{0.98}Na_{0.02})(12DAP)_{0.7}C_{11}$
6	2.75 (Li), 0.66 (Na)	25.2	$(Li_{0.93}Na_{0.07})(12DAP)_{0.8}C_{15}$
10	2.05 (Li), 0.53 (Na)	26.7	$(Li_{0.93}Na_{0.07})(12DAP)_{1.1}C_{19}$
24	2.18 (Li), 3.79 (Na)	24.2	$(Li_{0.66}Na_{0.34})(12DAP)_{0.7}C_{12}$

Na−12DAP−GIC (d_i = 0.749 nm). As shown in Table 2, Li content decreases, and Na content increases, as the reaction proceeds.

The continuous change in lattice dimension vs the Li content [x, in $Li_xNa_{1-x}(12DAP)_yC_z$] follows Vegard's law for solid solutions, Figure 8. Composition-dependent lattice variations,

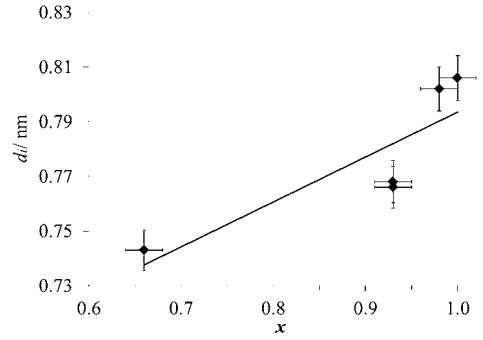

Figure 8. A plot of d_i of the first stage (Li,Na)−12DAP−GIC vs the Li content x as in $(Li_xNa_{1-x})(12DAP)_yC_z$. The y-error bars for d_i show ±1 standard deviation. The x-error bars are ±0.01.

either linear or with anomaly, were reported for $K_{1-x}Rb_xC_8$.[57−59] In the present case, Li metal reacts with 12DAP rapidly, forming the Li^+−12DAP complex that intercalates initially. This is clear from the optimized reaction times of 6 h vs 72 h for preparation of Li− and Na−12DAP−GIC, respectively (see the Experimental Section). The Li^+ complex is slowly displaced by Na^+−12DAP as reaction times increase. Li^+−12DAP can also displace the Na^+ complex in a prepared Na−12DAP−GIC sample (data not shown), suggesting there is little thermodynamic preference for either complex and that reaction kinetics and mass action play a dominant role in this exchange. In addition to $M(12DAP)_y^+$ (M = Li, Na) complexes, the $Na(EN)_y^+$ complexes can also be exchanged with tetra-alkylammonium cations,[60] resulting in a new route to novel GICs.

To our knowledge, the only other quaternary GIC of this type reported is $Hg(benzene)_2C_8$ (M = K, Rb),[28] which forms ordered heterostructures as opposed to the solid solutions described above.

Quaternary GICs with Two Amine Intercalates. When stage 2 Na−EN−GIC [d_i = 0.678 nm, Figure 9a] reacts with Na metal and 12DAP, the solid changes from black/blue to intense blue. The PXRD patterns for the obtained products are shown in Figure 9b−d. A stage 1 quaternary Na−(EN,12DAP)−GIC (d_i = 0.716 nm) is observed with a gallery dimension intermediate between Na−EN−GIC (0.691 nm) and Na−12DAP−GIC (0.749 nm). At long reaction times,

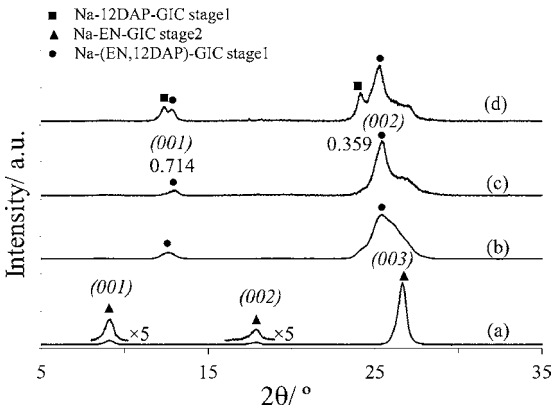

Figure 9. The PXRD patterns of (a) stage 2 Na−EN−GIC and the product from its reaction with Na metal and 12DAP at (b) 6, (c) 24, and (d) 72 h. The d values (in nm) and assigned Miller indices (00L) are indicated for each reflection.

Na−12DAP−GIC appears in addition to Na−(EN,12DAP)−GIC.

There is no diffraction evidence for an ordered heterostructure where the EN-solvated Na^+ intercalates into alternate galleries. We propose that $Na(12DAP)_y^+$ complexes intercalate into both the empty layer and the layer already occupied by $Na(EN)_y^+$. The displacement reaction occurs more slowly than the opening of new galleries, accounting for the formation of a quaternary compound followed by appearance of the Na−12DAP−GIC phase. Attempts to prepare quaternary GICs by the reaction of graphite with Na and a mixture of EN and 12DAP (at several different ratios) yielded disordered materials, as indicated by broad PXRD patterns.

From the previously reported d_i values for Li−(BzN,THF)−GIC (d_i = 0.744 nm)[29] and K−(THF,Bz)−GIC (d_i = 0.9 nm),[30] organic cointercalates can form solid solutions. There have also been reports of ordered heterostructures for acceptor-type GICs, where the second guest species intercalates into the empty gallery easily without displacing the initial guest species.[61]

CONCLUSIONS

We described the synthesis and structure of M−diamine−GICs, employing the systematic investigation of diamines with different alkyl chain lengths, different positions of the $-NH_2$ group, and the presence of $-CH_3$ substituents. Stage 1 and 2 Li−EN−GICs show the first example of a monolayer perpendicular-to-parallel intercalate transition. The presence of methyl group(s) in 12DAP and DMEDA (i) inhibits that transition and (ii) enforces the chelation to Li^+ in the GICs. Two examples of cation-directed orientation of organic cointercalates in GICs are identified, in the series M−12DAP−GIC (M = Li, Na, and K) and M−EN−GIC (M = Li, Na). In these cases, the GICs with the smaller-radius cation show greater gallery expansions.

We also reported the synthesis of quaternary GICs containing mixed metal cations or mixed amines. (Li,Na)−12DAP−GIC was synthesized through the one-pot synthesis, showing a variation in gallery height dependent on reaction time and the composition. Na−(EN,12DAP)−GIC, on the other hand, was prepared from the preformed stage 2 Na−EN−GIC and shows an invariant gallery height.

dx.doi.org/10.1021/ic201661y | Inorg. Chem. 2011, 50, 11676−11682

AUTHOR INFORMATION

Corresponding Author

*Phone: +1 541 737 6747. Fax: +1 541 737 2062. E-mail: michael.lerner@oregonstate.edu.

ACKNOWLEDGMENTS

Part of this work was presented at 2010 Solid State Chemistry Gordon Research Conference. T.M. thanks OSU Chemistry and the Gordon Research Conference for financial support.

REFERENCES

(1) Whittingham, M. S.; Jacobson, A. J. *Intercalation Chemistry*; Academic Press: New York, 1982.
(2) Ogawa, M.; Kuroda, K. *Bull. Chem. Soc. Jpn.* **1997**, *70*, 2593.
(3) Han, S. S.; Jang, S. S. *Chem. Commun.* **2009**, 5427.
(4) Zhao, Y. F.; Kim, Y. H.; Simpson, L. J.; Dillon, A. C.; Wei, S. H.; Heben, M. J. *Phys. Rev. B* **2008**, *78*, 144102.
(5) Osada, M.; Sasaki, T. *J. Mater. Chem.* **2009**, *19*, 2503.
(6) Inagaki, M. *J. Mater. Res.* **1989**, *4*, 1560.
(7) Viculis, L. M.; Mack, J. J.; Kaner, R. B. *Science* **2003**, *299*, 1361.
(8) Shioyama, H. *Tanso* **2010**, *241*, 6.
(9) Catheline, A.; Valles, C.; Drummond, C.; Ortolani, L.; Morandi, V.; Marcaccio, M.; Iurlo, M.; Paolucci, F.; Penicaud, A. *Chem. Commun.* **2011**, *47*, 5470.
(10) Valles, C.; Drummond, C.; Saadaoui, H.; Furtado, C. A.; He, M.; Roubeau, O.; Ortolani, L.; Monthioux, M.; Penicaud, A. *J. Am. Chem. Soc.* **2008**, *130*, 15802.
(11) Widenkvist, E.; Boukhvalov, D. W.; Rubino, S.; Akhtar, S.; Lu, J.; Quinlan, R. A.; Katsnelson, M. I.; Leifer, K.; Grennberg, H.; Jansson, U. *J. Phys. D Appl. Phys.* **2009**, *42*, 112003.
(12) Novikov, V. P.; Kirik, S. A. *Tech. Phys. Lett.* **2011**, *37*, 565.
(13) Solache-Rios, M.; Garcia-Sosa, I.; Sosa-Reyes, S. *J. Radioanal. Nucl. Chem.* **1998**, *237*, 151.
(14) Herrera-Alonso, M.; Abdala, A. A.; McAllister, M. J.; Aksay, I. A.; Prud'homme, R. K. *Langmuir* **2007**, *23*, 10644.
(15) Dresselhaus, M. S.; Dresselhaus, G. *Adv. Phys.* **2002**, *51*, 1.
(16) Setton, R. Ternary Systems. In *Graphite Intercalation Compounds I. Structure and Dynamics*; Zabel, H., Solin, S. A., Eds.; Springer-Verlag: Germany, 1990.
(17) Solin, S. A.; Zabel, H. *Adv. Phys.* **1988**, *37*, 87.
(18) Rüdorff, W. *Adv. Inorg. Chem. Radiochem.* **1959**, *1*, 223.
(19) Merle, G.; Letoffe, J. M.; Rashkov, I. B.; Claudy, P. *J. Therm. Anal.* **1978**, *13*, 293.
(20) Maluangnont, T.; Gotoh, K.; Fujiwara, K.; Lerner, M. M. *Carbon* **2011**, *49*, 1040.
(21) Setton, R.; Beguin, F.; Facchini, L.; Quinton, M. F.; Legrand, A. P.; Ruisinger, B.; Boehm, H. P. *J. Chem. Soc., Chem. Commun.* **1983**, 36.
(22) Rüdorff, W. *Chimia* **1965**, *19*, 489.
(23) Stumpp, E.; Alheid, H.; Schwarz, M.; Janssen, J. J.; Müller-Warmuth, W. *J. Phys. Chem. Solids* **1996**, *57*, 925.
(24) Scharff, P.; Alheid, H. *Phys. Status Solidi A* **2000**, *177*, 93.
(25) Skipper, N. T.; Walters, J. K.; Lobban, C.; McKewn, J.; Mukerji, R.; Martin, G. J.; de Podesta, M.; Hannon, A. C. *J. Phys. Chem. B* **2000**, *104*, 10969.
(26) Maluangnont, T.; Bui, G. T.; Huntington, B. A.; Lerner, M. M. *Chem. Mater.* **2011**, *23*, 1091.
(27) Maluangnont, T.; Sirisaksoontorn, W.; Lerner, M. M. 2011, [Online] DOI: 10.1016/j.carbon.2011.09.018
(28) Isaev, Y. V.; Guerard, D.; Blumenfeld, A. L.; Lenenko, N. D.; Novikov, Y. N. *Carbon* **1996**, *34*, 97.
(29) Ginderow, D. *Ann. Chim.* **1971**, *6*, 5.
(30) Hamwi, A.; Touzain, P.; Bonnetain, L. *C. R. Acad. Sci., Ser. II* **1984**, *299*, 1385.
(31) Kargina, I.; Richeson, D. *Chem. Mater.* **1996**, *8*, 480.
(32) Figueroa, E.; Brill, J. W.; Selegue, J. P. *J. Phys. Chem. Solids* **1996**, *57*, 1123.
(33) Schmidt, C.; Rosen, M. E.; Caplan, D. F.; Pines, A.; Quinton, M. F. *J. Phys. Chem.* **1995**, *99*, 10565.
(34) Moreh, R.; Pinto, H.; Finkelstein, Y.; Beguin, F. *J. Phys. Chem. Solids* **1996**, *57*, 909.
(35) Schlögl, R.; Boehm, H. P. *Carbon* **1984**, *22*, 341.
(36) Liau, Y. H.; Su, T. M. *J. Am. Chem. Soc.* **1992**, *114*, 9169.
(37) Kimmel, T.; Becker, D. *J. Org. Chem.* **1984**, *49*, 2494.
(38) Delville, A.; Detellier, C.; Gerstmans, A.; Laszlo, P. *Helv. Chim. Acta* **1981**, *64*, 556.
(39) Rocher, N. M.; Frech, R.; Powell, D. R. *J. Phys. Chem. B* **2006**, *110*, 15117.
(40) Mizutani, Y.; Ihara, E.; Abe, T.; Asano, M.; Harada, T.; Ogumi, Z.; Inaba, M. *J. Phys. Chem. Solids* **1996**, *57*, 99.
(41) Abe, T.; Mizutani, Y.; Tabuchi, T.; Ikeda, K.; Asano, M.; Harada, T.; Inaba, M.; Ogumi, Z. *J. Power Sources* **1997**, *68*, 216.
(42) Cousins, D. M.; Davidson, M. G.; Garcia-Vivo, D.; Mahon, M. F. *Dalton Trans.* **2010**, *39*, 8203.
(43) Melero, C.; Guijarro, A.; Yus, M. *Dalton Trans.* **2009**, 1286.
(44) Rhine, W. E.; Stucky, G. D. *J. Am. Chem. Soc.* **1975**, *97*, 737.
(45) Mackenzie, F. M.; Mulvey, R. E.; Clegg, W.; Horsburgh, L. *Polyhedron* **1998**, *17*, 993.
(46) Sanders, R. A.; Frech, R.; Khan, M. A. *J. Phys. Chem. B* **2003**, *107*, 8310.
(47) Armstron, D. R.; Graham, D. V.; Kennedy, A. R.; Mulvey, R. E.; O'Hara, C. T. *Chem.—Eur. J.* **2008**, *14*, 8025.
(48) Bock, H.; Havlas, Z.; Hess, D.; Nather, C. *Angew. Chem., Int. Ed. Engl.* **1998**, *37*, 502.
(49) Jordan, V.; Behrens, U.; Olbrich, F.; Weiss, E. *J. Organomet. Chem.* **1996**, *517*, 81.
(50) Janiak, C. *Chem. Ber.-Rec.* **1993**, *126*, 1603.
(51) Dye, J. L. *Acc. Chem. Res.* **1968**, *1*, 306.
(52) Wotiz, J. H.; Barelski, P. M.; Hinckley, C. C.; Koster, D. F.; Kleopfer, R. D. *J. Org. Chem.* **1972**, *37*, 1758.
(53) Beguin, F.; Pilliere, H. *Carbon* **1998**, *36*, 1759.
(54) Goldmann, M.; Beguin, F. *Phase Trans.* **1991**, *30*, 91.
(55) Duc, C. M.; Mai, C.; Rivière, R.; Golé, J. *J. Chim. Phys. Phys.-Chim. Biol.* **1972**, *69*, 991.
(56) Zhao, Y. H.; Abraham, M. H.; Zissimos, A. M. *J. Org. Chem.* **2003**, *68*, 7368.
(57) Solin, S. A.; Chow, P.; Zabel, H. *Phys. Rev. Lett.* **1984**, *53*, 1927.
(58) Medjahed, D.; Merlin, R.; Clarke, R. *Phys. Rev. B* **1987**, *36*, 9345.
(59) Chow, P. C.; Zabel, H. *Phys. Rev. B* **1988**, *38*, 12837.
(60) Sirisaksoontorn, W.; Adenuga, A. A.; Remcho, V. T.; Lerner, M. M. *J. Am. Chem. Soc.* **2011**, *133*, 12436.
(61) Shioyama, H. *Syn. Met.* **2000**, *114*, 1.